

FEM model of induction hardening of gear of mixture material

J. Hodek ^{a *}, P. Shykula ^b

^a COMTES FHT, Prumyslova 995, 334 41, Dobrany, Czech Republic

^b Miba, Nabrezie Oravy 2222, Dolny Kubin, Slovakia

* Corresponding e-mail address: josef.hodek@comtesfht.cz

ABSTRACT

Purpose: The purpose of this article is to describe the construction of an FEM model for computing residual stresses generated by induction hardening of a high-carbon steel gear.

Design/methodology/approach: The 3D FEM model comprised two parts. The first one which dealt with induction heating was prepared using MSC Marc commercial software. The second one, a model of temperature and deformation fields, was developed with the aid of DEFORM 3D commercial software. Material data was considered to be temperature-dependent. In the second part of the model, the material data was defined on the mixture basis: a separate temperature-dependent data set was specified for each phase, including transformation rules. The data was obtained in part by measuring and in part by calculation using JMatPro commercial software. Temperatures during heating and cooling were measured by means of thermocouples. The convection heat transfer coefficient was determined and the model of induction heating validated using the measured data. The thickness of the martensitic layer upon heat treatment was measured to validate the model.

Findings: The 3D FEM model described here predicts the temperature distribution during heat treatment and the thickness of the martensitic layer upon heat treatment accurately. It was thus deduced that this material model was defined correctly and that the calculation of residual stresses would correspond to the reality.

Practical implications: Future work should focus on refining the model, e.g. on incorporating transformation plasticity and on analysing the relationship between the residual stress distribution upon heat treatment and the part's fatigue.

Originality/value: The material model described in this article takes into account phase transformations which have a substantial impact on the post-treatment distribution of residual stresses. The 3D FEM model with this type of definition of material provides good predictions of residual stress distribution in the gear.

Keywords: Gear hardening; Induction heating; Finite element method (FEM); Residual stresses; Mixture material

Reference to this paper should be given in the following way:

J. Hodek, P. Shykula, FEM model of induction hardening of gear of mixture material, Journal of Achievements in Materials and Manufacturing Engineering 71/2 (2015) 87-92.

ANALYSIS AND MODELLING

1. Introduction

The quenching of steel which leads to rapid thermally-induced transformation of austenite to martensite is an important metallurgical process. This microstructural change leads to volume changes which, in turn, alter the distribution of stresses in the workpiece. Generally, the resulting stress distribution tends to be non-uniform. By varying induction heating parameters, one can obtain various residual stress distributions in gears upon heat treatment, and thus alter their mechanical properties.

Mathematical modelling of induction heat treatment of gears [1-4] helps to optimise process parameter values in order to achieve prime quality products. Such calculations are typically carried out using Ansys, Abaqus, Marc, Deform and other commercial software packages, as well as user subroutines. Although a great deal of the resulting residual stress is due to the transformation of austenite to martensite, a number of calculations fail to take this fact into account.

The main purpose of this work was to construct a 3D FEM model capable of describing with sufficient accuracy the residual stresses that result from induction heat treatment of a gear, while taking into account the microstructure of the gear material and related phase transformations.

2. Development of mathematical model

An FEM model was constructed to describe the residual stress that exists in a gear after induction heat treatment. Thanks to the gear's symmetry, only one quarter of a gear tooth was considered. The model comprised two parts linked by a Python script.

2.1. Induction heating

The first part was concerned with induction heating and the resulting temperature fields. It was developed using the commercial MSC Marc finite-element software. Coupled magnetodynamic-thermal analysis brings together harmonic magnetodynamic analysis and thermal analysis. First, a harmonic magnetodynamic analysis is performed which is then followed by a thermal analysis. The harmonic magnetodynamic field generates induced currents in the model. These induced currents generate heat and a heat flux is computed which is then used in the thermal analysis. The temperature dependency of material data was taken into account. The induction current and frequency were

considered to be constant values. The mesh of the gear accounted for the skin depth, i.e.: the depth at which the magnitude of the induced current density drops to e^{-1} of the magnitude at the surface. The mesh on the surface of the gear comprised at least three elements per skin depth. The magnetodynamic field is described by equations for the vector A and scalar V potentials [5] where μ stands for the magnetic permeability, ω is angular frequency and γ denotes electrical conductance:

$$\text{curl}(\mu^{-1} \text{curl } A) + \gamma(j\omega A + \nabla V) = 0 \quad (1)$$

$$\nabla[\gamma(j\omega A + \nabla V)] = 0 \quad (2)$$

The transient temperature field is expressed by the Fourier equation [5]:

$$c\rho dT/dt = \nabla(\lambda \nabla T) + w \quad (3)$$

Here, c denotes specific heat, ρ stands for density, λ is thermal conductivity and w represents the heat loss during induction heating.

2.2. Quenching and stress

In the second part, temperature and strain fields were studied using the DEFORM 3D commercial software package, taking into account the microstructure of the material. The gear was considered to be of a mixture material. A mixture is defined as a system made up of material phases. Material data and transformation relations are defined for each material phase.

In this second part of the model, the temperature field is represented by equation (3). The w value is zero because there is no current in the induction coil and therefore no heat source.

The object is an elastic-plastic body.

An incremental strain [6] is assumed to consist of several components:

$$d\epsilon = d\epsilon^E + d\epsilon^\Theta + d\epsilon^P + d\epsilon^{Tr} \quad (3)$$

The upper indices E, Θ , P and Tr denote elastic, thermal, plastic and phase-transformation components of strain. When introducing the temperature and structure-dependent yield function $F = f(\sigma_{ij}, \epsilon_{ij}, T)$, the plastic strain rate, elastic strain rate, and thermal strain rate, can be expressed in the following forms:

$$\dot{\epsilon}_{ij}^P = \lambda \frac{\partial F}{\partial \sigma_{ij}} \quad (4)$$

$$\dot{\epsilon}_{ij}^E = \frac{1+\nu}{E} \dot{\sigma}_{ij} - \frac{\nu}{E} \dot{\sigma}_{kk} \delta_{ij} \quad (5)$$

$$\dot{\epsilon}_{ij}^T = \alpha(T - T_0) \delta_{ij} \quad (6)$$

Here, λ is a positive proportionality constant, ν is the Poisson's ratio, E is the Young's modulus, δ_{ij} is the Kronecker's delta, T is the temperature, T_0 is the temperature of the previous step and α is the thermal expansion coefficient.

During the heat treatment, some phase transformations may take place. The phase transformations lead to material volume changes due to changes in the metal's structure. The transformation strain is used mainly to account for the structure change during the transformation and is in the form of:

$$\dot{\epsilon}_{ij}^{Tr} = \sum \beta_l \dot{\zeta}_l \delta_{ij} \quad (7)$$

Where β_l is the strain coefficient for the transformation from one phase to another and $\dot{\zeta}_l$ is the transformation volume fraction rate.

2.3. Python script

The two parts of the computational model were linked by a user subroutine in the Python environment. It exported the temperature distribution in the gear after induction heating calculated by MSC Marc into DEFORM 3D.

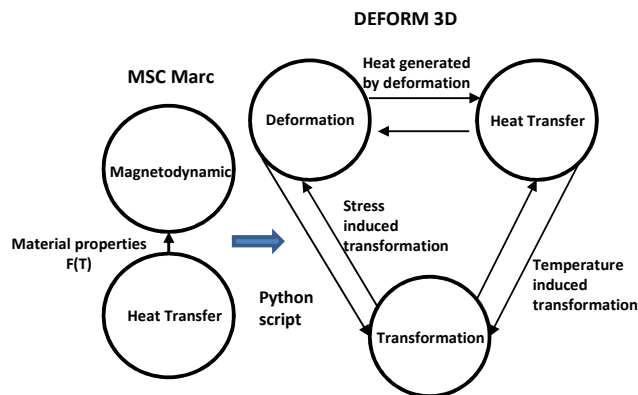


Fig. 1. Computational procedure

The latter tool was then used for simulating the cooling process, taking into account phase transformations taking place in the gear. The entire computational procedure is illustrated in Fig. 1.

3. Material data

An L75PT dilatometer was used for thermal expansion Measurement. The austenitizing temperature was determined from the thermal expansion distribution. The value was increased by approximately 20 % for the use in the FEM model. This corresponds to very rapid temperature changes. LFA1000 laser flash equipment was used to determine heat transfer properties: specific heat, and thermal diffusivity as a function of temperature. Thermal conductivity was computed from thermal diffusivity and measured density.

The rest of the material property data needed was determined using the JMatPro software. JMatPro is simulation software which calculates a wide range of material properties on the basis of chemical composition. It is particularly focused on multi-component alloys used in industrial practice. From the chemical composition of the gear material, the following temperature-dependent data was calculated: electrical conductivity for computing the induction heating process, the Young's modulus, Poisson's ratio and flow stresses for all components of the mixture.

This mixture material model contains four phases: pearlite, austenite, martensite and bainite. The initial phase in the model is pearlite. Transformation rules govern the relationships between these individual phases. The following transformations [6] are defined for the computation:

Austenite→bainite: diffusional transformation

$$\dot{\zeta} = 1 - e^{-bt^n} \quad (8)$$

Where: ζ is the volume fraction transformed, t denotes time, and b and n are transformation parameters.

Austenite→martensite: martensitic transformation

The parameters defined include the transformation start temperature T_s , and 50 % martensite level temperature T_{50}
 Pearlite→austenite: diffusional transformation of the same type as in (8)

Volume change and latent heat change are defined as temperature-dependent curves for all above-listed transformations.

4. Measurements of temperature and martensitic layer thickness

Temperature profiles during heating and cooling were measured for several combinations of power and time. Thermocouples were used for the Measurement (see Fig. 2).



Fig. 2. Temperature measurement

At every instant, four temperatures were measured simultaneously: at two points at the top of the tooth and at two points at its bottom. Average values were then calculated from the temperatures of the tooth top and bottom. Those values should be understood to be approximations because it was not possible to weld the thermocouples onto exactly same locations. During the temperature measurement, the gear was not revolving.

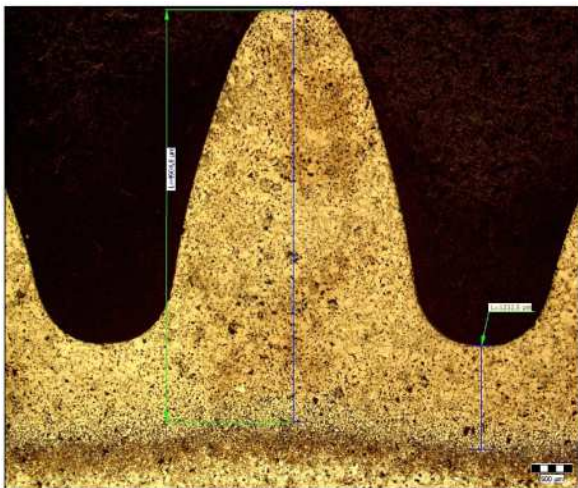


Fig. 3. Martensitic layer after heat treatment

The thickness of the martensitic layer was measured in the symmetry plane of the gear. An example of the shape of the martensitic layer is shown in Fig. 3.

5. FEM model

As the problem is geometrically symmetrical, the computational model only comprised one quarter of a single tooth (see Fig.).

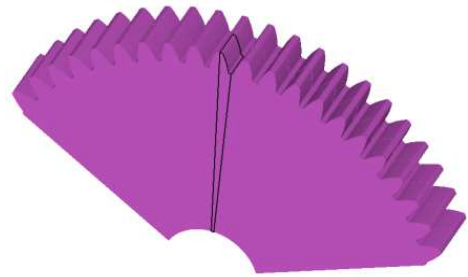


Fig. 4. Model of the gear - one quarter of the gear tooth

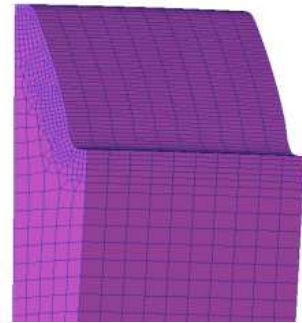


Fig. 5. The detail of the meshed gear

The model was meshed so that it comprised at least three elements across the skin depth (see Fig. 5).

Induction heating - the models of the magnetodynamic and thermal fields in the MSC Marc software comprised the gear, the inductor and a sufficiently large portion of the environment. The boundary conditions were set for magnetodynamic field on the surface to [5]:

$$\partial A / \partial n = 0 \text{ and } A = 0, V = const \quad (9), (10), (11)$$

in the case of symmetry and fixed potential, respectively.

The boundary conditions were set for thermal field on the gear surface to [5]:

$$\partial T / \partial n = 0 \text{ and } -\lambda \partial T / \partial n = \alpha (T - T_a) \quad (12), (13)$$

in the case of symmetry and Newton boundary condition, respectively. Here, α is the convection coefficient and T_a is the ambient temperature. In the case of induction heating, the convection coefficient was set to a constant value of $20 \text{ W/m}^2\text{K}$.

The quenching process - the calculation of stresses, temperatures and transformations in DEFORM 3D - only involved the gear. Relevant displacement restrictions were defined on the surface of the gear as the boundary conditions for the stress computation [6]:

$$u_{i,j,k} = 0 \quad (14)$$

Here, u is the movement in appropriate direction i, j or k .

The boundary conditions for the thermal field have the same character as (12) and (13). The only difference is the convection coefficient. The convection coefficient α was determined by inverse heat transfer analysis as a function of the surface temperature (see Fig. 4).

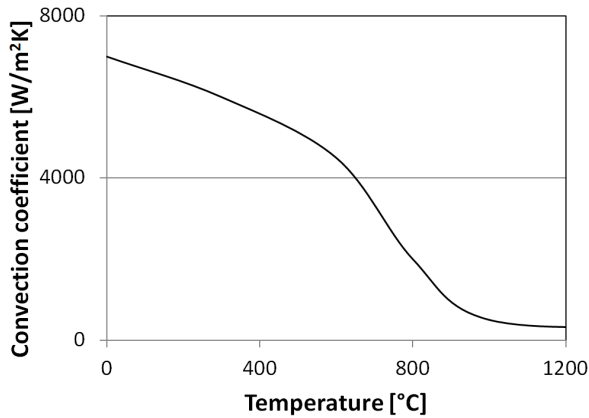


Fig. 6. Convection coefficient for the quenching process

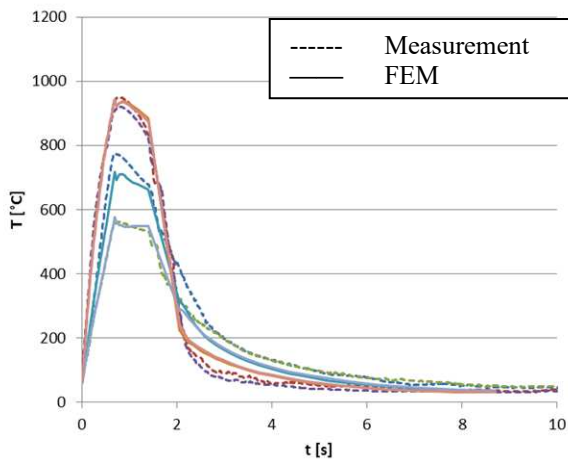


Fig. 7. Example of comparison between calculated and measured temperatures

The model was set up using the measured data in order to correspond to the real-world processes that take place during heat treatment. The inductor current was varied until the measured and calculated temperatures were in sufficient agreement (see Fig. 7).

The diffusional transformation model and the martensitic transformation model were varied until the measured and calculated martensitic layer data were in sufficient agreement (see Fig. 8).

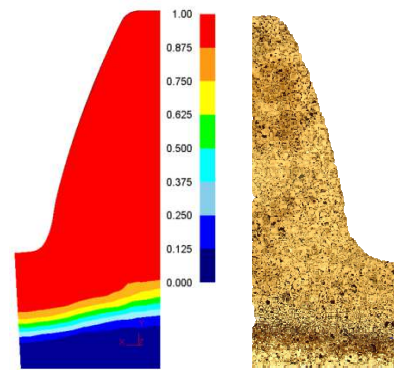


Fig. 8. Comparison between calculated and measured shape of the martensitic layer

6. Results and Discussion

Using the above-described FEM model, the post-heat treatment residual stress distribution was calculated for the following gear parameters:

Diameter/module D=90mm/1.5mm
 Frequency/power f=150kHz / 85kW
 Heating/cooling time $t_h=0.8$ s / $t_c=8$ s

The temperature of the tooth upon heating (see Fig. 9) is between 1000 and 1200°C. The temperature field is non-uniform. As a consequence of the skin effect, the highest-temperature location is the top of the tooth in the plane of symmetry. The temperature of the tooth root is approximately 1000°C.

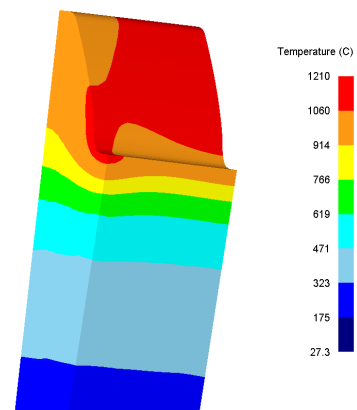


Fig. 9. Temperature distribution after heating

The region where the temperature is sufficiently high becomes austenitized (see Fig. 10).

The progress of the martensitic transformation and the distribution of effective stress during cooling are shown in

Figures 11 12, respectively. The extent of the martensite layer formed upon cooling corresponds to the austenite region after heating. The reason is that the layer is relatively thin and cools down rapidly. All austenite therefore transforms to martensite.

Residual stress represented by effective stress upon cooling is illustrated in the right part of Fig. 12. The maximum value can be found at the root of the tooth.

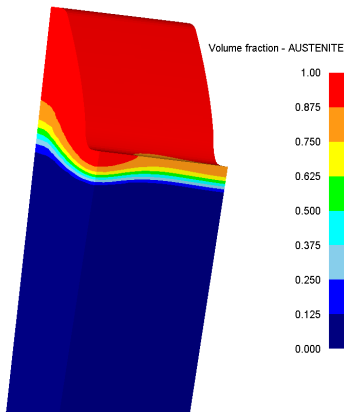


Fig. 10. Austenite distribution after heating

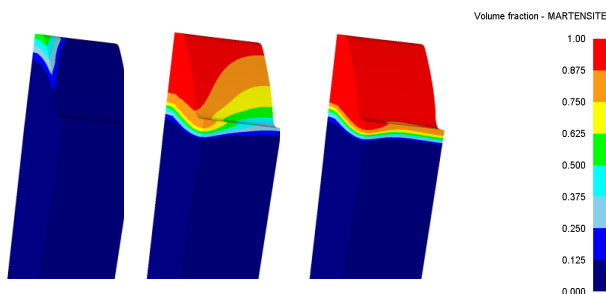


Fig. 11. The progress of martensitic transformation for 2s, 3s and 8 seconds into the cooling process

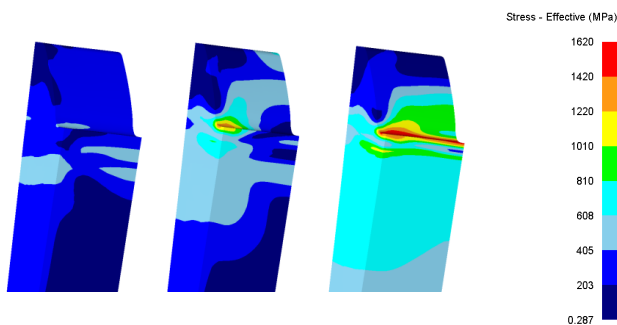


Fig. 3. Effective stress of the process and for 2s, 3s and 8 seconds into the cooling process

7. Conclusions

The above-described FE model characterises the behaviour of gears during surface hardening. The model integrates calculations of electromagnetic, temperature and strain parameters and accounts for phase transformations. The model was set against measured temperatures and the thickness of the martensitic layer. Temperature-dependent material properties were in part measured and in part calculated. Using the FE model, one can estimate the behaviour of the gear during heat treatment, namely the time profiles of temperature, phase and stress distribution.

In their follow-up research, the authors will focus on the relationship between the residual stress distribution and the contact fatigue resistance of gears.

Acknowledgements

This study was carried out under a project entitled “Development of West-Bohemian Centre of Materials and Metallurgy” No.: LO1412 which is funded by the Ministry of Education of the Czech Republic.

References

- [1] J. Barglik, A. Smalcerza, R. Przyluckia, I. Doležel, 3D modeling of induction hardening of gear wheels, *Journal of Computational and Applied Mathematics* 270 (2014) 231-240.
- [2] J. Montalvo-Urquizo, Q. Liu, A. Schmidt, Simulation of quenching involved in induction hardening including mechanical effects. *Computational Materials Science* 79 (2013) 639-649.
- [3] P. Šuchman, J. Hodek, Optimization of Induction Hardening Parameters through FEM Simulation, *Proceedings of the 20th IFHTSE Congress, 2012, Beijing.*
- [4] J. Hodek, FEM simulation induction heating process, *Proceedings of the 23th International Conference on Metallurgy and Materials, METAL'2014, Czech Republic.*
- [5] Theory and User Information, Marc 2014, Volume A, 331.
- [6] Deform v11.0.2 System Documentation.